Application of Weibull Probability to Predict the Size of Inclusion in Metallic Material

by

Megat Atif Bin Megat Shahair

Dissertation submitted in partial fulfilment of

the requirements for the

Bachelor of Engineering (Hons)

(Mechanical Engineering)

JULY 2008

Universiti Teknologi PETRONAS
Bandar Seri Iskandar
31750 Tronoh
Perak Darul Ridzuan

CERTIFICATION OF APPROVAL

Application of Weibull Probability to Predict the Size of Inclusion in Metallic Material

By

Megat Atif Bin Megat Shahair

A project dissertation submitted to the

Mechanical Engineering Programme

Universiti Teknologi PETRONAS

in partial fulfillment of the requirement for the

BACHELOR OF ENGINEERING (Hons)

(MECHANICAL ENGINEERING)

Approved by,

_____

(Assoc. Prof. Dr. Faiz Ahmad)

UNIVERSITI TEKNOLOGI PETRONAS

TRONOH, PERAK

July 2008

CERTIFICATION OF ORIGINALITY

This is to certify that I am responsible for the work submitted in this project, that the original work is my own except as specified in the references and acknowledgements, and that the original work contained herein have not been undertaken or done by unspecified sources or persons.

3/10/2008

_____

MEGAT ATIF BIN MEGAT SHAHAIR

ABSTRACT

Large inclusions can be the initiation site for fatigue failure in metal components. As melting processes are becoming more refined, the size of the inclusions falls below the level of detectability of the non-destructive testing methods. This final year project is divided into three parts. In the first part of the project, Weibull probability was applied to predict largest oxide inclusion size and compare to the actual observation under scanning electron microscope. The results showed that Weibull probability prediction is accurate with margin of ± 3 microns. In the second part of project, the Weibull probability was tested using nodular cast iron. The nodules were measured for their true and apparent sizes, respectively. Based on the data, the effect on Weibull probability was found to be negligible. In the third part of the project, rotating fatigue test was performed under cantilevered loading by using two sets of medium carbon steel specimens. The specimens were annealed at 840 °C, held for one hour and furnace cooled before being polished and tested. Step-size method was selected where each specimen was subjected to 2.52×10^5 cycles at initial load of 5 N. The load was increased progressively until the specimen eventually fails. Only those specimens failed due too oxide inclusion at fatigue initiation site were regarded. Based on observational results, the two sets had different probability of survival which corresponded to their respectively largest oxide inclusion size.

ACKNOWLEDGEMENT

In the completion of this final year project, it is impossible to complete without the tremendous cooperation from a lot of people. I am extremely grateful to those people who had contributed their time, moral support and resources for me. The gratitude goes to my supervisor, Assoc. Prof. Dr. Faiz Ahmad, who helped and guided me throughout the research tenure.

Of course to my parents who never failed to support me through the ups and downs of life. Without your prayers and concern, I would not be able to persevere to the end. To my fellow friends, I am grateful to have very helpful and cooperative people around me.

大家，很多谢谢。
爸爸妈妈，我爱你们。
Megat Atif Megat Shahair
[二零零八年十二月三日]

TABLE OF CONTENT

CHAPTER 3 PROJECT WORK

CHAPTER 4 RESULT AND DISCUSSION

CHAPTER 5 CONCLUSION

REFERENCES

APPENDICES

LIST OF FIGURES

LIST OF TABLES

CHAPTER 1

INTRODUCTION

1.1 BACKGROUND OF STUDY

Improvements of steelmaking technology over the last decades have led to gradual reduction of oxide inclusions content in steel. With limited solubility of oxygen in solidified steel, steelmakers use total oxygen content as an adequate measure of the total oxide inclusions present in steel. Steel cleanliness acts as a measure of total oxide inclusions and rated through various inclusion rating methods like ASTM E45 Methods or Jernkontorets Inclusion Rating.

Today's steelmakers are striving for higher cleanliness, hoping that the oxide inclusions decrease as well. It is true that higher cleanliness means lower oxide content, but unfortunately, this does not necessarily means good fatigue strength.

1.2 PROBLEM STATEMENT

1.2.1 Problem Identification

Inclusions issue is of great concern because it decreases engineering steel fatigue strength. The improvement in internal cleanliness in terms of oxide inclusion is remarkable that nearly zero rating is achieved in the industry. Even with good cleanliness rating, failure analysis repeatedly indicates that most application using these steels had inclusion at fatigue fracture origins.

1.2.2 Significance of Project

It is relevant to bearing steels, spring steels and tool steels manufacturing industries as these steel components are subjected to cyclic loading. The fatigue strength of those parts is seriously affected by oxide inclusions.

1.3 OBJECTIVES AND SCOPE OF STUDY

1.3.1 Objective

The main objectives of this research are:

1. To validate the prediction of Weibull probability method for estimating the maximum oxide inclusion in steel, and the effect of sample sectioning on the probability.

2. To analyze the accuracy of the above method by fatigue testing.

1.3.2 Scope of Study

The scope of studies for this project is limited to globular-shaped oxide inclusions in steel product only. Quantitative evaluation of the inclusion cleanliness is prepared for data collection. The data is then analyzed using statistical analysis of Weibull probability and extrapolated to represent the actual product. This data will be compared with the actual laboratory results. Fatigue testing is subsequently done to test the statistical analysis.

1.4 FEASIBILITY OF THE STUDY

Feasibility of Idea

The idea of the study is obtained from books and journals as cited in the reference. The most prominent author in bringing up this idea is Y. Murakami (Professor at Department of Mechanical Science and Engineering, Kyushu University). The probability technique is well-accepted academically as the underlying concept is quite feasible, but it is yet to be applied extensively in the steelmaking industry.

Feasibility of Work Completion

The two major factors that dictate the feasibility of completing this study are timely delivery of materials and availability of apparatus.

CHAPTER 2

LITERATURE REVIEW / THEORY

2.1 Introduction

Inclusions in simplest explanation are unwanted particles in material that adversely affecting its properties. Even with the latest technology, inclusions are inevitable introduced during steelmaking [4]. The quantification of inclusions based on standard inclusion ratings is done with respect to dispersion, shape, chemical composition and morphology. For fatigue strength application, this is inadequate as inclusion critical size and the probability of sample not cutting to the center of the inclusion are not being addressed.

Various types of inclusions in steel are oxide, titanium (in form of titanium carbonitride), sulphur (in form of manganese sulphide) and calcium (in form of duplex inclusions) [4], but this study will be limited to oxide only.

2.2 Variation of Cleanliness Terminology

The term 'clean steel' is commonly used to describe steels that have [9]:

   a. Low levels of solute elements like sulfur, phosphorous, nitrogen, oxygen and hydrogen;

   b. Controlled levels of residual elements like copper, lead, zinc, nickel, magnesium and chromium;

   c. Low frequency of product defects which related to presence of inclusions.

This is quite a big range to be covered in one terminology. In order to deal with the variable, it is better to define '*high purity steel*' as steels with low levels of solutes and '*low residual steels*' as steels with low level of impurities from scrap melting. In addition, '*clean steels*', as the main focus of this study, are steels with low frequency of product defect.

2.3 Steel Production

Before proceeding further, the understanding of the steel production is important. There are basically two different methods of steel production namely the converter process and the electric arc furnace process. For both processes oxygen is blown to remove carbon where carbon and oxygen are reduced simultaneously forming carbon monoxide gas.

Liquid steel easily picks up gases of hydrogen and nitrogen up to equilibrium content. By blowing of argon through the melt, partial pressure is reduced and consequently lowers both hydrogen and nitrogen. The required partial pressure of degassing depends on other elements as well; for example, removal of nitrogen is improved if sulphur is very low or chromium is high [7].

When Al is added for further *deoxidation*, inclusions rise quickly into the top slag due to different density between the inclusions and the melt. The slag and inclusions can be removed easily after melt down.

Al content however causes a risk of *reoxidation*. Newly formed residual Al_2O_3 is in solid form and may coagulate together with old residual to clog the nozzle. This solid Al_2O_3 must be modified to liquid calcium aluminates by Ca addition. As Ca has higher reactivity than Al, it will react with Al_2O_3 forming a liquid-mixed oxide [8].
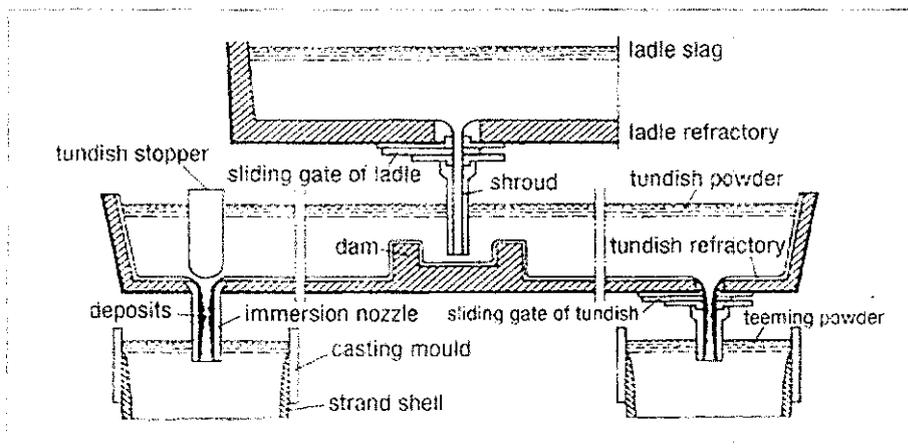
Figure 1: Locations that Oxide may be introduced in Continuous Casting [8]

After metallurgical treatment, most melts are transferred to the continuous caster machine. They are teemed through the refractory lined tundish into the mould. A shroud protects the teeming stream from ladle to the tundish from risk of air contamination. Both the shroud and the immersion nozzle are air-tight.

Special powders are added to the melt surface to minimize heat radiation loss and are capable of absorbing inclusions. This teeming powder must also avoid possible adhesion to the mould by forming a thin slag shell between melt and mould.

At the start, liquid steel streams into the empty tundish while the metal surface is yet to be completely protected with tundish powder. The liquid steel may react with the remaining air in the mould [8]. Therefore, the initial part of the teeming strand has higher inclusion content than the later part.

2.4 Super Clean Steel Production

Super-clean involves a special treatment to create steel with low inclusions content. The inclusions, that are not feasible to remove, should be elongated during rolling (ductile inclusion) or broken to small particles with soft edges (brittle inclusion). Some guidelines for super clean steel production:

   i.   The hot metal should have low contents of elements that segregate at grain boundary like phosphorus, tin, arsenic or antimony [8].
   ii. Dissolved oxygen must be transformed into solid or gas before casting [8].
   iii. External source of oxygen must be eliminated.
   iv. Refractories must be chemically inert to the liquid steel.

2.5 Source of Oxide Inclusions

Oxides are identified to be formed either from a deoxidation product (primary inclusions) or created during solidification (secondary formation inclusions) or by reoxidation (tertiary inclusions) with ladle / tundish refractory, with top slag, with casting powder or with penetrated air.

6

2.6 Cleanliness Sampling

Cleanliness sampling is ideally made on the steel final product. Sampling can also be done earlier in the process by taking liquid metal out of the ladle or the tundish to estimate the total oxygen content. The latter technique is merely as indication of expected cleanliness level due to errors because:

1. Inclusions may be modified along by reaction with ladle refractory or with the ladle slag.

reoxidation

$$\frac{1}{2}\{O_2\} + 2(Fe)^{2+} = (O)^{2-} + 2(Fe)^{3+}$$
$$(O)^{2-} + 2(Fe)^{3-} = [O] + 2(Fe)^{2+}$$

boundary steel/slag

$$(CaO) + [S] + \tfrac{2}{3}[Al] = (CaS) + \tfrac{1}{3}(Al_2O_3)$$
$$(SiO_2) + \tfrac{4}{3}[Al] = [Si] + \tfrac{2}{3}(Al_2O_3)$$
$$(FeO) + \tfrac{2}{3}[Al] = [Fe] + \tfrac{1}{3}(Al_2O_3)$$
$$(CaC_2) + 2(O) = (CaO) + 2\{CO\}$$
$$(Ca) + [S] = (CaS)$$
$$(SiO_2) + 2(Ca) = [Si] + 2(CaO)$$

degassing

$$2[N] = \{N_2\}$$
$$2(H) = \{H_2\}$$
$$[C] + [O] = \{CO\}$$

boundary refractory/steel

$$<MgO> + \tfrac{2}{3}[Al] = \tfrac{1}{3}(Al_2O_3) + \{Mg\}$$
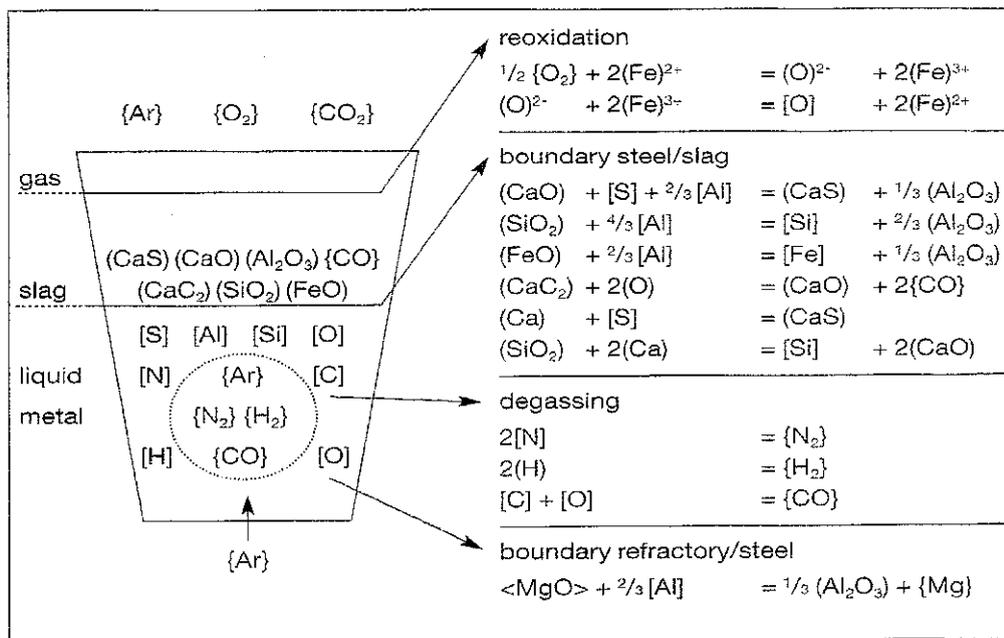
Figure 2: Possible Chemical Reactions of Steel in Ladle Refractory [8]

2. During rolling, inclusions may be broken down to smaller size.
3. Segregations appear during solidification. When molten steel containing impurities (like sulphur and phosphorus) or slag particles in suspension, they will be solidified last due to lower freezing point.

7
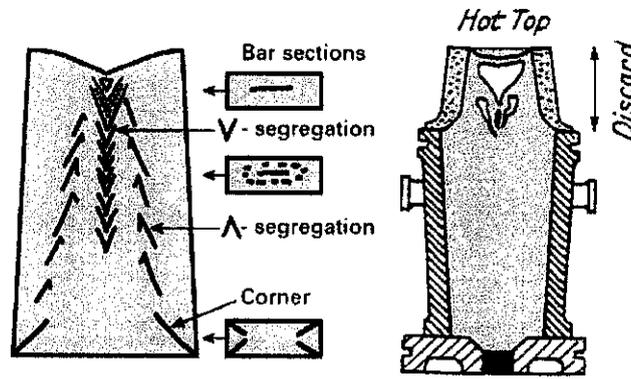
Figure 3: Segregation in Steel [10]

Segregations normally formed in the centre and upper portions of the ingot. Associated with the pipe, they are largely removed when it is discarded [10].

2.7 Steel Cleanliness and its Fatigue Properties

Steel oxygen content indicates the total oxide content because of its very limited solubility in solidified steel. The total oxide content is also known as steel cleanliness. High cleanliness means lower oxide content while low cleanliness means high oxide content.

According to Monnot's study [1a], there is no general rule that relates fatigue strength of steel to its cleanliness. Also, rotating-bending fatigue tests carried out by Adachi [1b] showed presence of rather large inclusions in the clean bearing steels which were graded 'clean' according to JIS. Adachi emphasized the importance of developing new method to find this kind of extremely large inclusion, which cannot be predicted using conventional inclusion rating methods.

Although an oxide of 50 µm diameter is big, one hundred inclusions of this size in 1 cm^3 contribute a content of merely 1 ppm of total oxide content. By decreasing oxide content but *not* reducing the size of oxide will result in no better fatigue limits. The problem is unsolved regardless of remarkable improvement of steel cleanliness.

8

Uhrus [1d] showed that only oxide inclusions more than 30 μm in diameter should be taken into account when evaluating fatigue strength of ball bearings. Duckworth and Ineson [1e] showed that inclusions smaller than threshold size did not affect fatigue strength, which is also similarly to the one reported by de Kazinczy [1f].

In one study [1a], the inclusion distribution of two steels produced by process A and B, obtained via visual inspection (see Figure 4), compares with diameters of oxides appearing at fatigue fracture origins, obtained from rotating-bending fatigue test. The idealization is presented in Figure 5.
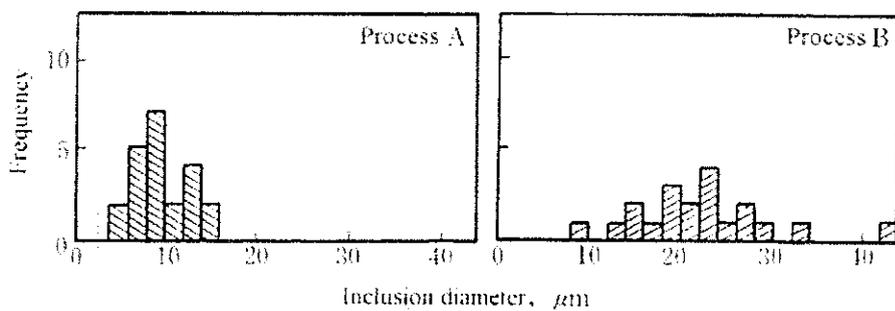
Figure 4: Frequency versus Inclusion Diameter in Steel A (Process A) and Steel B (Process B)
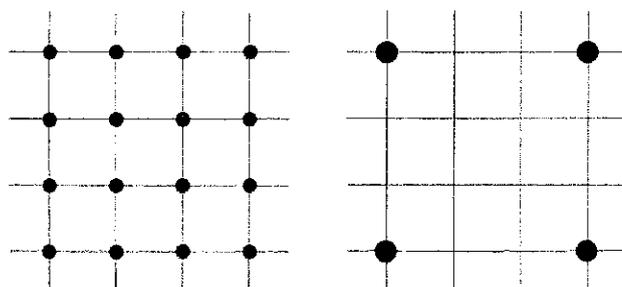
Figure 5: Idealized Representation of figure 4

16 small inclusions (left side), 4 large inclusions (right side), whose both volume are identical

The steel A contains more inclusions than steel, thus, rating indicates steel B is *cleaner* than steel A. However when tested, due to the size of inclusions of steel B are larger than steel A, fatigue strength of steel A is being *higher*.

2.8 The $\sqrt{area}$ parameter model

The value of threshold intensity factor (K_{th}) is dependent of defect size, so conventional fracture mechanics approach is not applicable [16]. In addition, the geometry of small defects is three-dimensional. Many models for small defects have been proposed, but they cover mostly simple geometries only.

For this situation, Murakami and Endo [17] proposed a geometrical parameter $\sqrt{area}$ which succeeded in deriving simple equation for predicting fatigue strength of steel containing small defects. This model is called the " $\sqrt{area}$ **parameter model**". The $\sqrt{area}$ is defined as the square-root of the area by projecting the small defect onto the plane perpendicular to the maximum tensile stress.

The proposed prediction equation of the fatigue strength of specimens with a small defect subjected to uniaxial cyclic loading under the stress ratio $R = -1$ [17]:

$$\sigma_w = \frac{1.43(HV + 120)}{\left(\sqrt{area}\right)^{\frac{1}{6}}}$$

where σ_w is the fatigue limit (MPa), HV is the Vickers hardness (kgf/mm^2) and $\sqrt{area}$ is a geometrical parameter (μm). Y. Murakami further extended the above equation for various values or stress ratio R. This equation enables one to predict the fatigue strength without a fatigue test.

2.9 Feasibility of Probability Utilization

2.9.1 Largest Inclusion Size

The Weibull probability is an applied statistical distribution for predicting the likelihood of an event given a set of past knowledge. This method is also known as the extreme value distribution probability. Murakami and co-workers [1c] have been applying Weibull distribution to predict largest size of inclusion of steel product based on a given sample.

In most exponential distributions, it is assumed that the function is constant over time. In other situation it is more realistic to suppose that the function either increases or decreases over time. The latter case is applicable to the study.

Since the distribution depends on parameters (α and β), we need to estimate the value by linearization using Least-Squared Method [14].

Weibull Cumulative Distribution Function:
$$F(x) = 1 - e^{-\alpha x^{\beta}}, x \geq 0$$

$$\ln(1 - F(x)) = -\alpha x^{\beta}$$

$$\ln\left(\frac{1}{1 - F(x)}\right) = \alpha x^{\beta}$$

$$\therefore \ln\ln\left(\frac{1}{1 - F(x)}\right) = \beta \ln x + \ln \alpha \qquad \xrightarrow{y = mx + c} \qquad \therefore Y = \beta \ln x + \ln \alpha$$

By using least-squared formula for slope, yielding

$$\beta = \frac{\sum_{j=1}^{n} x_j Y_j - \overline{x} \sum_{j=1}^{n} Y_j}{\sum_{j=1}^{n} x_j^2 - n(\overline{x})^2}$$

11

So, put the samples in ordered (smallest to biggest) by denoting $j = 1, 2, \ldots, n$

$$X_{(1)} < X_{(2)} < \ldots < X_{(n)}$$

and suppose that the data results in $X_{(j)} = x_{(i)}$, then using the fact that:

$$E[F(X_{(i)})] = \frac{j}{(n+1)} \longrightarrow \boxed{\textbf{Cumulative Distribution Function}}$$

True provided that whenever $X_{(j)}$ is the jth smallest of a sample size n from any continuous distribution F.

The cumulative distribution function will act as *the level of confidence* that we needed.

Recall that,
$$\therefore \ln\ln\left(\frac{1}{1-F(x)}\right) = \beta \ln x + \ln \alpha$$

Rearranging,
$$\ln[-\ln(1 - F(x))] = \beta \ln x + \ln \alpha$$

So for individual sample, approximates of $F(x_{(j)})$ by $E[F(X_{(j)})]$:

$$y_j = \ln[-\ln(1 - F(x_{(j)}))]$$

$$\therefore y_j = -\ln\left[-\ln\left(\frac{j}{(n+1)}\right)\right] \longrightarrow \boxed{\textbf{Reduced Variate}}$$

The reduced variate function approximates *the linearity of Weibull distribution*.

2.9.2 Inclusion True versus Apparent Shape
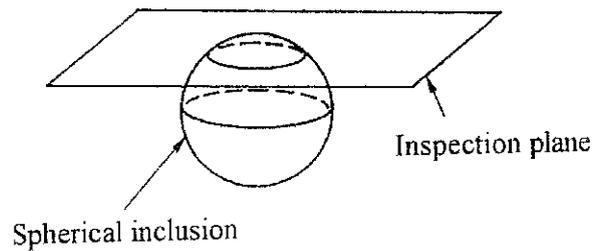
Figure 6: Sectioning Spherical Inclusion versus Inspection Plane [1]

When a planar section is cut for sampling preparation, inclusions are rarely cut through the centers but mostly at any other position. Inclusion is further refined in term of location namely surface inclusion, inclusion in touch with surface, and internal inclusion; all exhibit different fatigue strength values. The Weibull probability as discussed above (section 2.8.1) might be affected and this needs to be addressed as well using appropriate inclusion modeling, like regarding nodular cast iron as a model of inclusions [1g].

13

2.10 Assessment of Steel Cleanliness

There are several ways to determine oxide inclusions in steel sample. The two of them are [13]:

a. Micrographic Method (Jernkontoret and ASTM)
   - The observed sample fields are compared with the standard diagram and allocating them the classification of the diagram that resemble them closely.
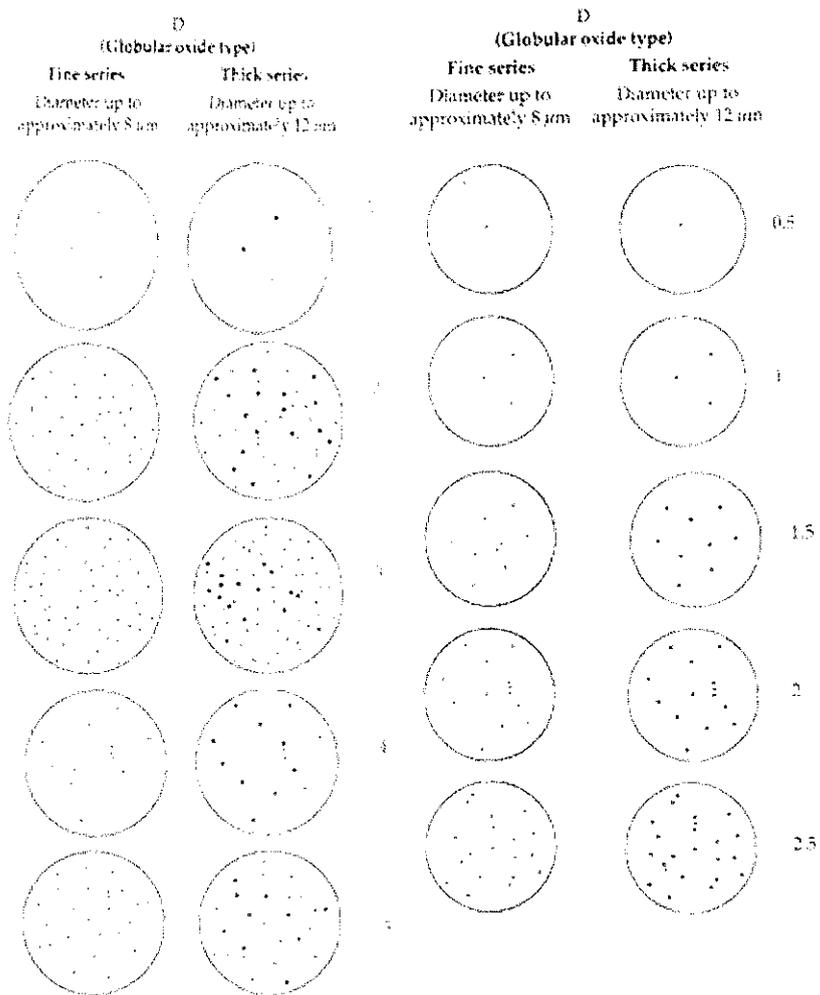
Figure 7: Standard Diagram of Jernkontoret (left) and ASTM (right)

b. Macrographic Method (ISO and JIS)

- The method of assessing inclusions by determining the total number and distribution of inclusions visible on the surface of fracture which has undergone blue tempering.

0		No inclusion with a length > 1 mm
1		Few very short stringers
2		Several very short stringers
3		Few very short stringers and short stringers
4		Several short stringers
5		Several short stringers and very short stringers
6		Several short stringers and one long stringer
7		Few long stringers and very short stringers
8		Several long stringers
9		Several long thick stringers
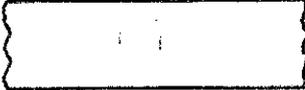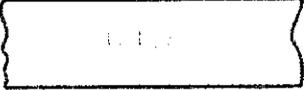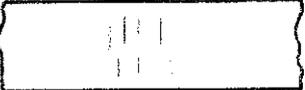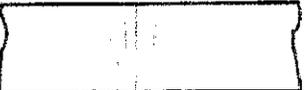
Explanation of terms
Very short stringers : ≥ 1 mm ≤ 2.5 mm   Few   : ≤ 3
Short stringers   : > 2.5 mm ≤ 5 mm   Several : > 3
Long stringers   : > 5 mm   Thick   : > 0.5 mm

Figure 8: Standard Diagram of ISO for Blue Fracture Test

CHAPTER 3

PROJECT WORK & METHODOLOGY

3.1 Project Activities

The project activities are mainly divided to two major parts of (i) investigating the probability techniques, and (ii) fatigue testing. The work flowchart is as follows:

```
                    ┌─────────────────────────┐
                    │    Literature Review    │
                    └─────────────────────────┘
                                │
                    ┌─────────────────────────┐
                    │    Experimental Work    │
                    └─────────────────────────┘
                      │                     │
          ┌───────────────────┐   ┌───────────────────┐
          │     Weibull       │   │  Fatigue Testing  │
          │   Probability     │   │     (Part C)      │
          └───────────────────┘   └───────────────────┘
            │             │
  ┌─────────────────┐ ┌─────────────────┐
  │  Under normal   │ │ Effect of       │
  │   condition     │ │ sectioning      │
  │    (Part A)     │ │   (Part B)      │
  └─────────────────┘ └─────────────────┘

                    ┌─────────────────────────┐
                    │  Experiment Validation  │
                    └─────────────────────────┘
                                │
                    ┌─────────────────────────┐
                    │       Discussions       │
                    └─────────────────────────┘
```
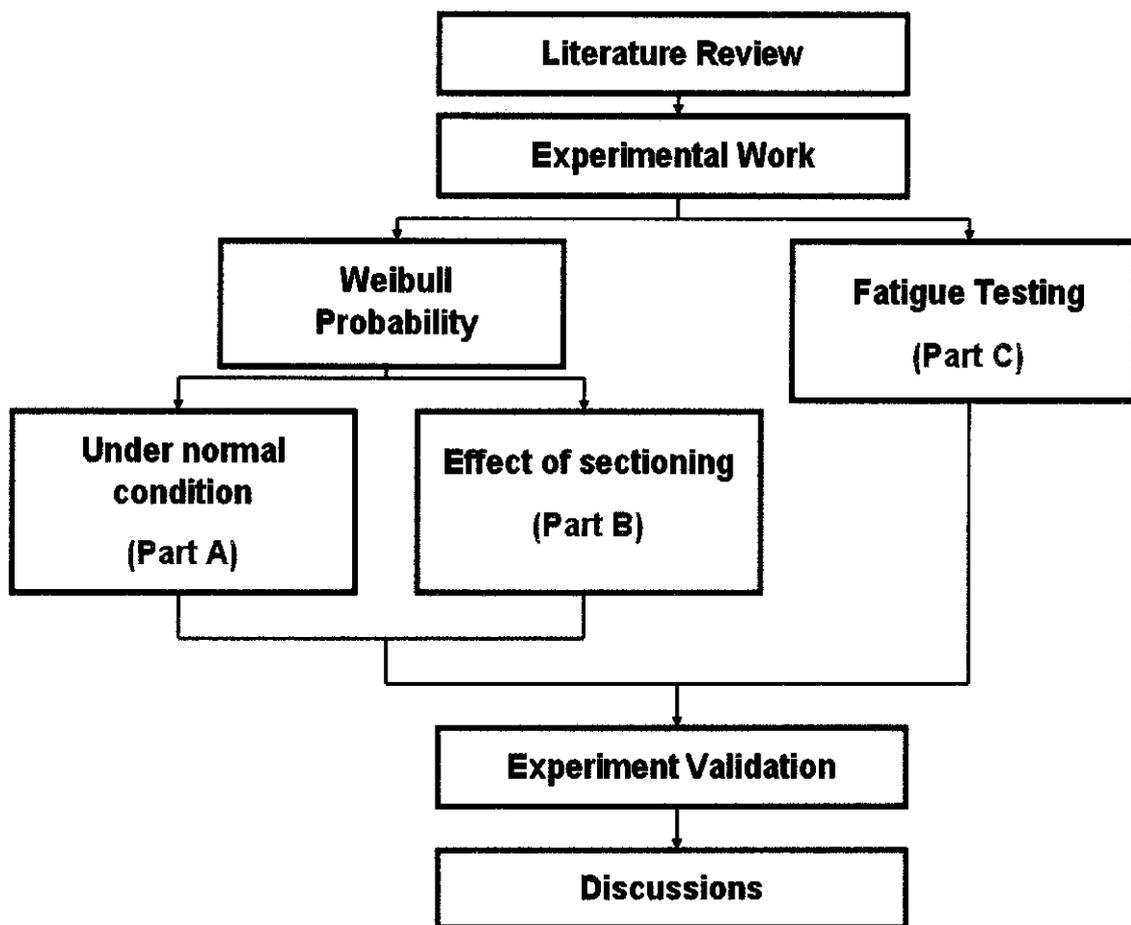
Figure 9: Experimental Flowchart

16

3.2 Methodology

3.2.1 Part A

Overview of Idea: If the total area can be inspected, this will yield the best result for detection of largest oxide inclusion size. Steel final product might be very big or in complex shape so it is usual to take a small sample area for practicality; but this is not without setback. Small sample area is prone to misrepresentation (see Figure 10) as the largest inclusion normally falls outside the sample area.
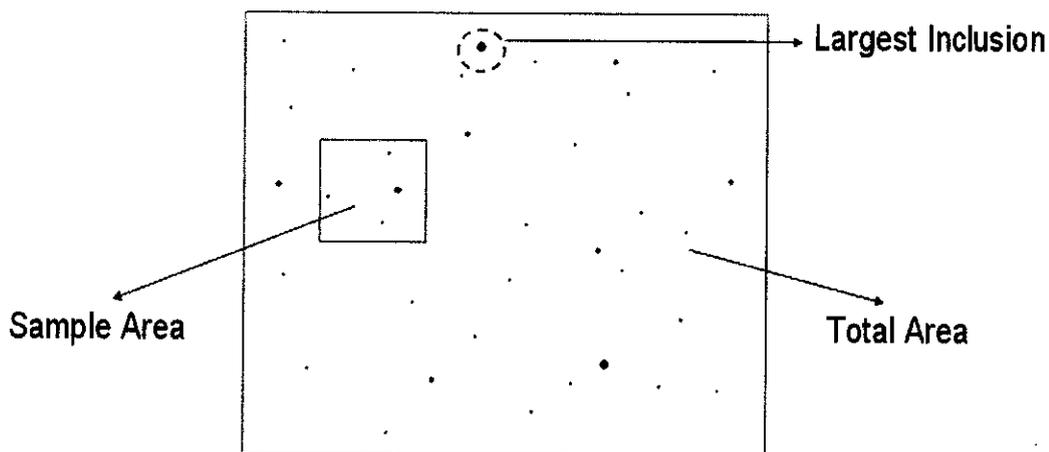
Figure 10: Idealization of Oxide Inclusion in One Inspection Plane

By introducing Weibull probability, the sizes of oxide inclusions in the sample area are collected and, based on those data, the largest oxide inclusion size can be predicted. In this project, the accuracy of Weibull probability is being investigated. This is done by comparing the actual result versus with the result by prediction of Weibull probability.

The acceptance criterion is that the largest oxide size must not exceed critical size. In general the thinner the product is, the smaller the critical oxide size. For example, oxide inclusion that is subjected to remote stresses, the critical size should not exceed 30μm [1d, 1e, 1f].

17

Methodology for largest inclusion size determination:

1. Check the samples chemical composition using SEM-EDS.
2. Prepare the steel samples:

   Procedure of Inspection:

   i. The fractured surface of steel product from blue fracture test (fracturing the steel and then tempered blue to increase the visibility of oxides) is examined. This section will be the total area S_1. The largest inclusion in S_1 is photographed and the inclusion diameter is measured. This is for reference purpose.

   ii. The sample area of S_0 is fixed and taken from the S_1. The largest inclusion in S_0 is photographed and the inclusion diameter is measured.

3. Perform Weibull probability of predicting presence of largest inclusion in each sample.

   Procedure of Weibull Probability:

   i. The same section from the steel product is taken.

   ii. Standard inspection area of S_0 in mm^2 is fixed. Microscopic picture, under no more than 10x optical magnification, is taken for reference. In this area of S_0, an inclusion is selected. The square root of the projected area, $\sqrt{area_{inclusion,j}}$ is calculated. This is repeated n times on all other visible inclusions.

   iii. Arrange the values of $\sqrt{area_{inclusion,j}}$ from smallest to the largest and numbered with $j = 1, 2, ..., n$.

   iv. Calculate the cumulative distribution function (F_j in %) and reduced variates (y_j) using equations $F_j = j \times 100(n+1)$ and $y_j = -\ln\{-\ln[j/(n+1)]\}$.

   v. The data above are then plotted using Weibull probability paper. The best-fit-straight-line graph is drawn.

18

vi.   Then, the intended inspection area S_1 is set. Return period T is calculated from $T = S_1 / S_0$. The intersection between T and the best-fit-straight-line graph will predict the largest inclusion size in the specimen. For fatigue strength application, the largest inclusion shall not exceed 30 μm.

4. Compare results obtained from step 2 against step 3.

3.2.2 Part B

Overview of Idea: When sectioning is done, there is a high chance of the sectioning not crossing the center of the inclusion (see Figure 11). This is important to be investigated because the magnitude order of oxide inclusion is small. Minor changes may affect the result.

In order to test the effect of apparent oxide inclusion size on Weibull probability, the inclusions must be made to known size and in well-distributed manner. This is metallurgically very difficult to produce. With this in mind, it is suggested to use nodular cast iron by representing the nodules as inclusions [1g].
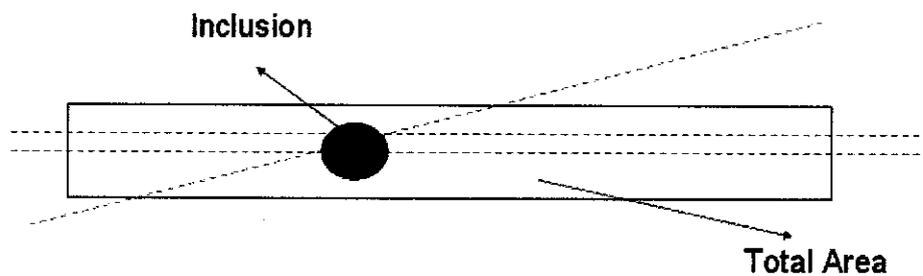
Figure 11: Inclusion with Several Sectioning Lines

Figure 12: Top View of Nodular Cast Iron

Apparent oxide inclusion size is defined as inclusion size measured when the sample is sectioned not through the center of the oxide inclusion. If it is sectioned through the center of oxide inclusion, it is known as true oxide inclusion size.
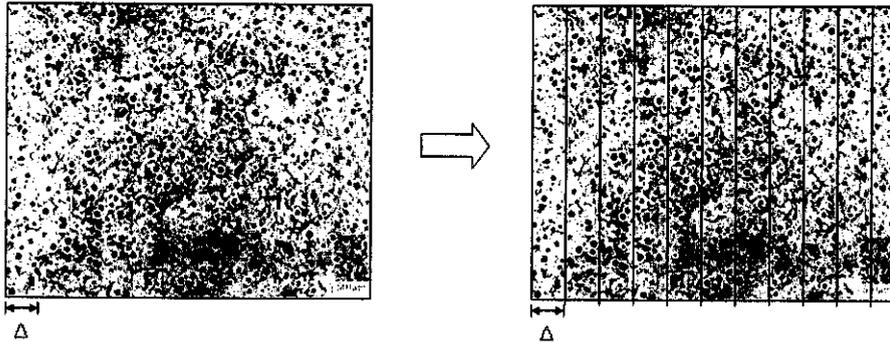
Figure 13: Modeling Inclusions using Nodular Cast Iron

By drawing equally-spaced lines, whereby each line passes only once on each individual nodule, the inclusion apparent sizes are measured as if the observer is looking from the side. Since the top view of the nodular cast iron can be seen (see Figure 12) the true inclusion size is directly known for each line. Weibull probability is then performed on both cases and the effect on the probability is examined.

Methodology for inclusion shape determination:
1. Metallographic samples of nodular cast iron are prepared.
2. By regarding the spheroidal graphite nodules as inclusion, microscopic photographs of sample are prepared. Equally spaced parallel lines are drawn with the condition that the two adjacent lines do not cross through the same single graphite nodule.
3. Procedure of Weibull probability is applied, except that $l_{max\_true,j}$ represents true maximum size of nodule while $l_{max\_apparent,j}$ represents apparent maximum size of nodule. All measurements are indexed with $j = 1, 2,..., J$. Weibull probability graph is then drawn.
4. Results obtained are evaluated.

21

3.2.3 Part C

Overview of Idea: Fatigue fracture is initiated by stress, in this case, at globular oxide inclusion (flaw). Once started at flaw, the edge of the crack acts as a stress-raiser and thus assists in propagation of the crack until final fracture.

This part is to prove the specimen that is labeled in Part A as having good or bad fatigue strength actually exhibits the expected outcome. This is demonstrated through classical fatigue experiment carried out by Wohler. His selection of reversing the stress on a specimen by employing a cantilever rotated about its longitudinal axis. This result in the stress at any point on the surface of the cantilever varies sinusoidally.
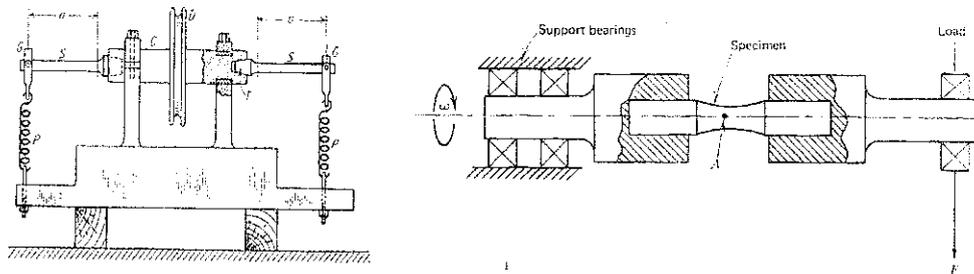
Figure 14: Rotating Fatigue Testing, Wohler model (left) and laboratory model (right)

Methodology for rotating fatigue testing:

1. As received, the diameters of the two sets of rolled bars were 10 mm and 12 mm, respectively. The sets were heat treated by annealing at 850°C for one hour and room temperature cooled after being shaped by lathe according to specimen dimension in Figure 22. It was then polished using sandpaper.

2. The specimen of each sets are loaded with predetermined stress (in MPa) and then the apparatus is started. The test is terminated either when the specimen fractures or it has reached beyond 10^5 cycles, whichever comes first. This is repeated until all specimens are completed.

3. Results obtained are evaluated.

22

3.3 Tool / Apparatus

Tool required for research completion:

1. Mechanical Apparatus: Rockwell Hardness and Fatigue Testing.

2. Micro-analysis: SEM-EDS.

3. Miscellaneous: Furnace, magnifying glass and optical microscope.
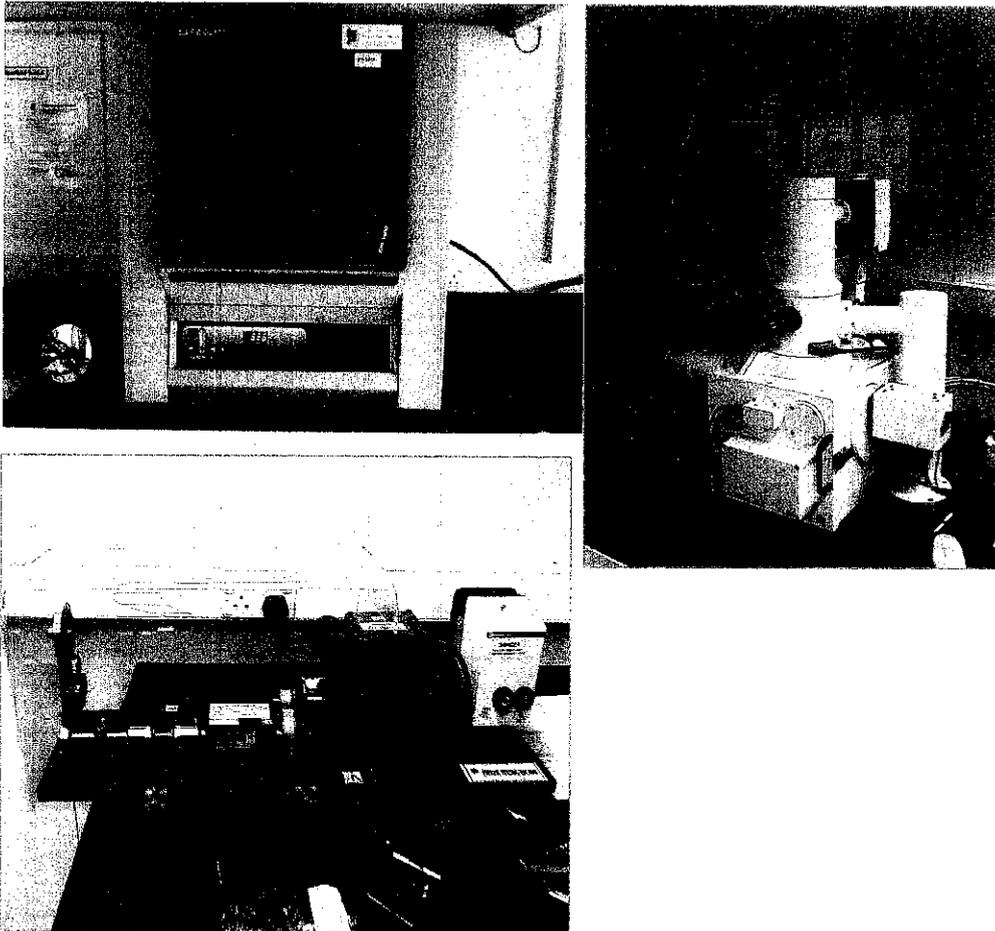
Figure 15: List of Equipments (top) Furnace, (right) SEM-EDS, (below) Fatigue Machine

CHAPTER 4

RESULTS AND DISCUSSIONS

4.1.1 Part A: Data Acquisition & Experiment Work
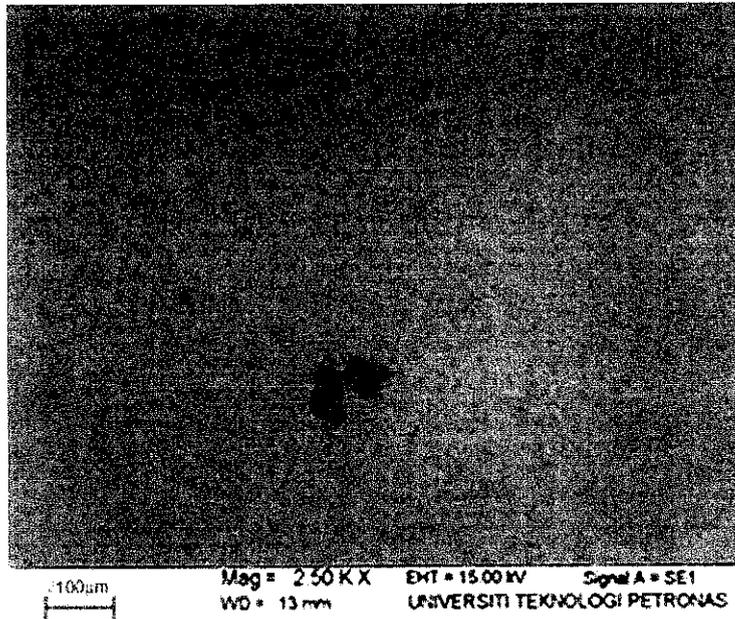
Figure 16: Largest Oxide Inclusion of Steel Sample A1
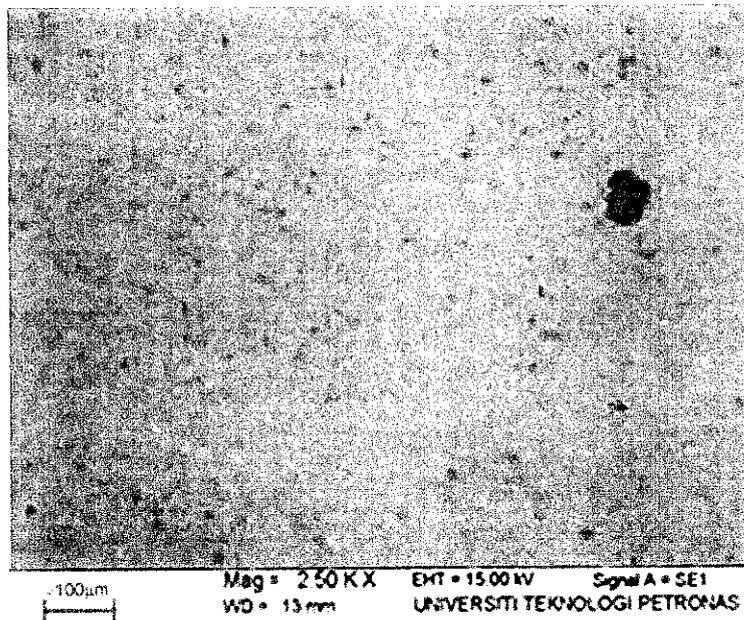
Figure 17: Largest Oxide Inclusion of Steel Sample A2
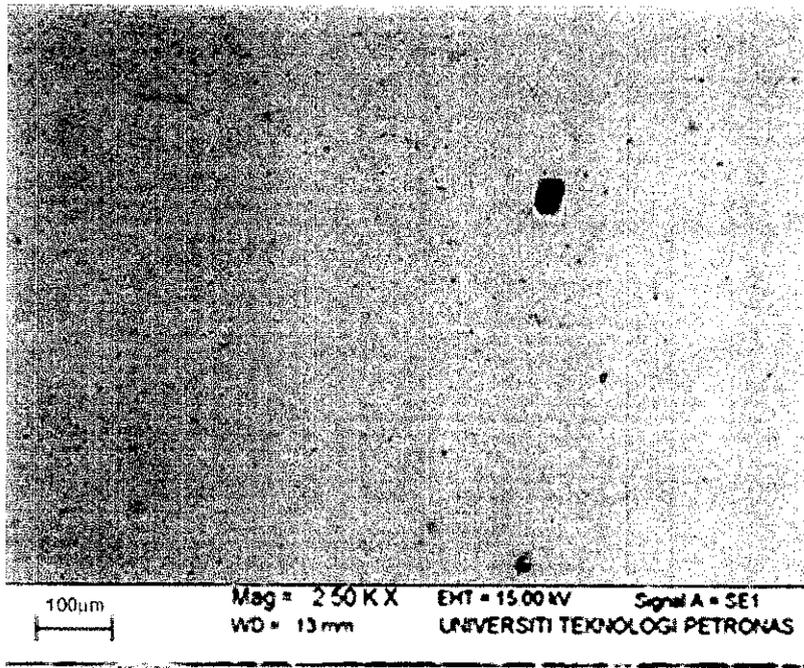
Figure 18: Largest Oxide Inclusion of Steel Sample A3
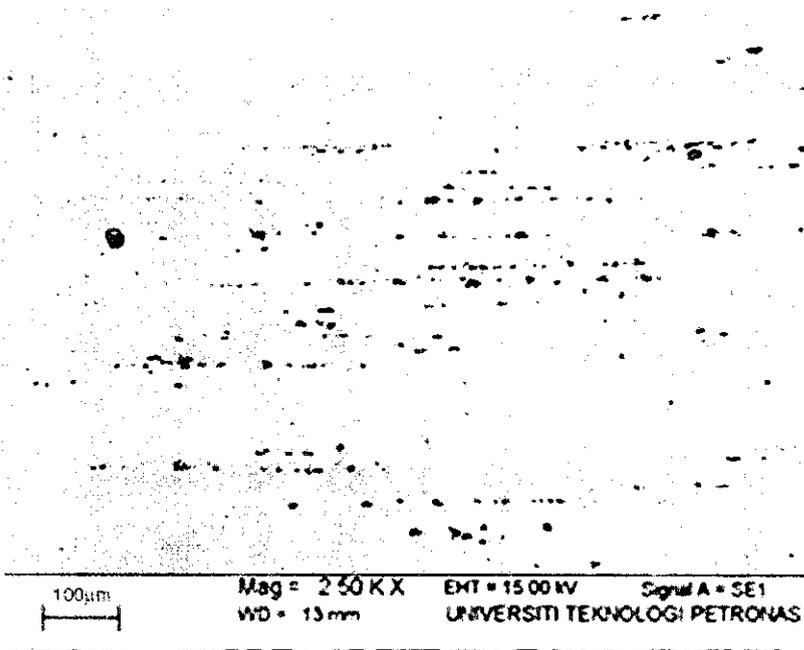
Figure 19: Largest Oxide Inclusion of Steel Sample A4

Table 1: Comparison between Predicted and Actual Largest Inclusion Size

Specimen Number	Predicted Largest Inclusion Size (μm) [From Weibull Probability]	Actual Largest Inclusion Size (μm) [From SEM Image]
A1	65	63
A2	66	63
A3	48	50
A4	40	38

4.1.2 Part A: Discussion

Surface of a metal sample is prepared and observed under optical microscope. Minimum twenty areas are chosen to be inspected at random. Each inspection size is of a standard size which is called as S_0. In this experiment it is set as 0.5 mm^2. The largest inclusion size for each area is measured, noted by $\sqrt{area}_{max}$. The Weibull Probability is plotted (cumulative function versus $\sqrt{area}_{max}$).

However, the procedure done is not necessarily accurate because:

(i) The largest inclusion size determined is <u>not</u> the *true* largest size because the observation plane may not be coincided with the actual plane of the inclusion diameter. This error is discussed in the next part (Part 4.2.1 - 4.2.2) of this final year project.

(ii) The assumption of only the inspected plane is applicable to the entire steel product may be too idealistic. This assumption, however, is tolerable for small product.

In order to prove the prediction is correct, the largest oxide inclusion for each steel samples are photographed and compared. From Table 1, the predicted size using Weibull probability is very close to the actual size. With this result, it can be concluded that the accuracy of Weibull probability is plausible.

4.2.1 Part B: Data Acquisition & Experiment Work

Figure 20: Modeling Inclusion Size for Weibull Probability (Sample B-1)
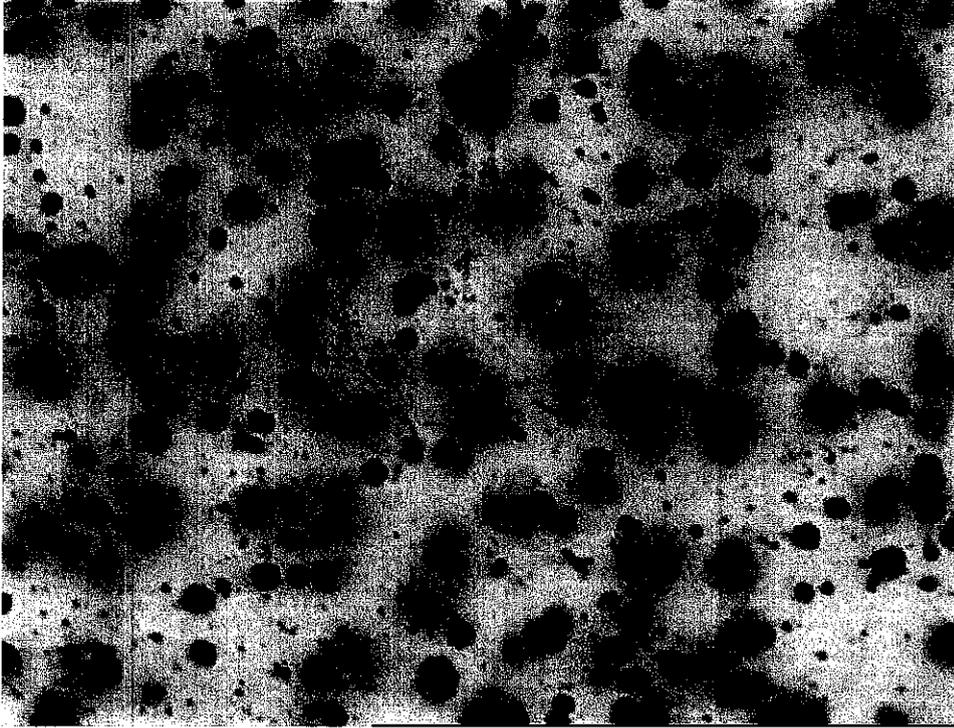
Table 2: Determination of Apparent and True Inclusion Size

Specimen Number	Apparent Size $l_{max\_apparent,j}$ (μ)	True Size $l_{max\_true,j}$ (μ)	Error (%)
B-1 **(Analysis 1)**	30	40	25.0
	42	55	23.6
	45	57	21.1
	48	60	20.0
	48	60	20.0
	60	65	7.7
	60	68	11.8
	60	68	11.8
	65	72	9.7
	68	76	10.5
	70	76	7.9
	73	76	3.9
	75	78	3.8
	77	78	1.3
	79	80	1.3
	78	82	4.9
	79	89	11.2
	84	92	8.7
	85	99	14.1
	89	100	11.0
	98	108	9.3
	104	111	6.3
	116	120	3.3
	120	125	4.0
	124	128	3.1

Table 3: Determination of Apparent and True Inclusion Size

Specimen Number	Apparent Size $l_{max\_apparent,j}$ (μ)	True Size $l_{max\_true,j}$ (μ)	Error (%)
B-1 (Analysis 2)	30	36	16.7
	38	42	9.5
	45	52	13.5
	48	52	7.7
	48	58	17.2
	54	60	10.0
	58	60	3.3
	62	62	0.0
	68	68	0.0
	70	78	10.3
	74	82	9.8
	74	88	15.9
	76	90	15.6
	80	90	11.1
	86	92	6.5
	90	98	8.2
	90	98	8.2
	90	102	11.8
	98	108	9.3
	100	112	10.7
	102	116	12.1
	104	120	13.3
	112	120	6.7
	118	124	4.8
	122	128	4.7

28

Figure 21: Modeling Inclusion Size for Weibull Probability (Sample B-2)
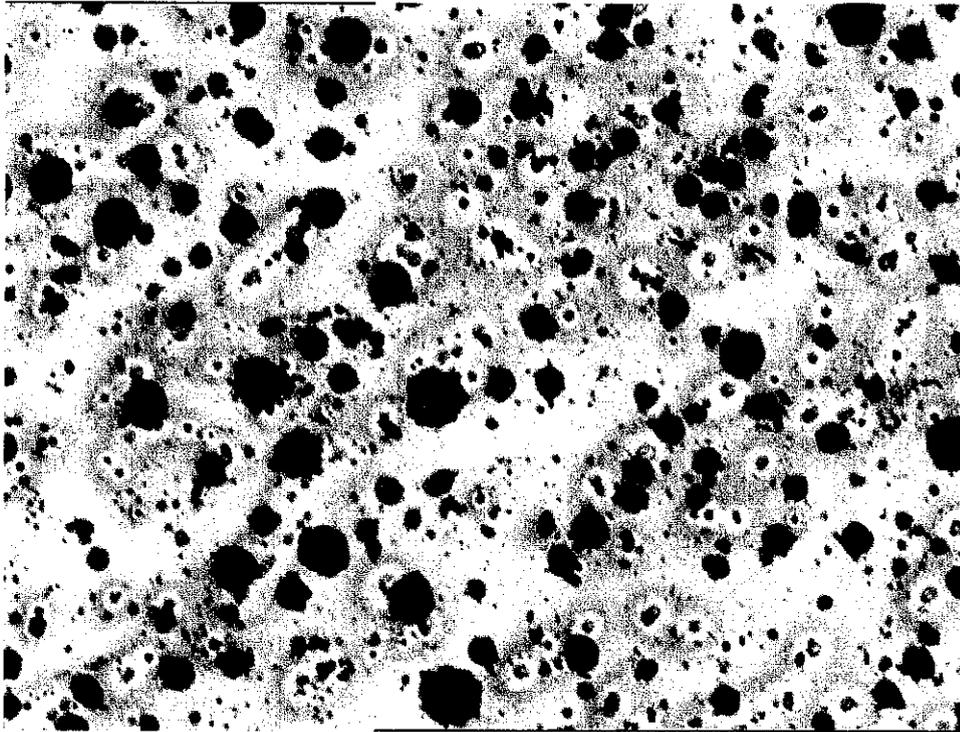
Table 4: Determination of Apparent and True Inclusion Size

Specimen Number	Apparent Size $l_{max\_apparent,j}$ (μ)	True Size $l_{max\_true,j}$ (μ)	Error (%)
B-2 (Analysis 1)	20	32	37.5
	24	44	45.5
	26	46	43.5
	26	50	48.0
	32	50	36.0
	43	54	20.4
	50	55	10.0
	55	59	6.8
	58	61	4.4
	61	73	16.4
	62	76	18.4
	73	76	3.9
	75	78	3.8
	78	78	0.0
	80	90	11.1
	82	95	13.7
	82	96	14.6
	85	96	11.5
	93	107	13.1
	94	108	13.0
	98	108	9.3
	101	111	9.0
	109	116	6.0
	111	121	8.3
	121	135	10.4

Table 5: Determination of Apparent and True Inclusion Size

Specimen Number	Apparent Size $l_{max\_apparent,j}$ (μ)	True Size $l_{max\_true,j}$ (μ)	Error (%)
B-2 (Analysis 2)	20	32	37.5
	22	32	31.3
	28	38	26.3
	29	38	23.7
	32	40	20.0
	40	55	27.2
	50	55	9.1
	55	59	6.8
	56	60	6.7
	62	70	11.4
	64	72	11.1
	73	76	3.9
	75	78	3.8
	78	78	0.0
	84	90	6.7
	84	95	11.6
	88	96	8.3
	90	96	6.3
	93	102	8.8
	98	108	9.3
	98	110	10.9
	104	111	6.3
	109	116	6.0
	112	120	6.7
	120	130	7.7

Table 6: Determination of Apparent and True Inclusion Size

Specimen Number	Apparent Size $l_{max\_apparent,j}$ (μ)	True Size $l_{max\_true,j}$ (μ)	Error (%)
B-2 (Analysis 3)	25	40	37.5
	28	42	33.3
	30	46	34.8
	30	48	37.5
	32	48	33.3
	38	52	26.9
	50	55	9.1
	55	59	6.8
	60	60	0.0
	62	70	11.4
	64	70	8.6
	70	76	7.9
	75	78	3.8
	78	82	4.9
	84	90	6.7
	84	95	11.6
	88	98	10.2
	90	100	10.0
	93	102	8.8
	98	112	12.5
	98	116	15.5
	112	120	6.7
	114	122	6.6
	120	128	6.3
	128	135	5.2

4.2.2 Part B: Discussion

Experiment Validation

Two metallographic set of nodular cast irons are prepared, labeled as sample B-1 (Figure 15) and B-2 (Figure 16) and observed under scanning electron microscope at a known magnification and scale. Two analyses were done on sample B-1 and another three on sample B-2.

Equally spaced parallel lines, known as inspection lines, are drawn on top of each photograph. The distance between the lines are chosen so that no two adjacent lines pass the same single nodule, this is to ensure the lines are not too close to one another and affecting the outcomes. The inspection lines cannot be shown in the Figure 15 and Figure 16 because the photographs are just partial of the whole plane.

The $l_{\max\_apparent,j}$, known as apparent maximum size, is defined as the longest line of the nodule being passed by the inspection line. The $l_{\max\_true,j}$, known as true maximum size, is defined as the largest measurable diameter of any nodule cut by the same inspection. All measurements are indexed with $j = 1, 2,.., J$, sorted from smallest to biggest, before the Weibull probability graph is plotted with best fit straight line drawn using Microsoft Excel. In addition, the apparent size and true size of nodules are also tabulated, and percentage error is calculated (% error = |true - apparent| / true x 100%). There are twenty five data for each analysis.

It should be noted that at zero percent and hundred percent cumulative distribution, the corresponding values of nodule size are not existed. At zero percent, it does not make any sense to have nodule size without level of confidence. At hundred percent, it is not quite right to say the probability data has the ultimate level of confidence. Hence, the range of the cumulative distribution function lies between 0.1 to 99.99 percent.

31

Experiment Results

Based on the result in Figure 17 to Figure 21, it can be seen that the differences between $l_{max\_apparent,j}$ and $l_{max\_true,j}$ is small on Weibull probability graph. Murakami [1] mentioned that since true maxima are always larger than the corresponding apparent maxima, the line of $l_{max\_true,j}$ is always to the right of the line $l_{max\_apparent,j}$. In addition, both of the lines should be parallel to each other. This can be clearly observed in all figures where the true size line (pink line) is on the right of the apparent size line (blue line).
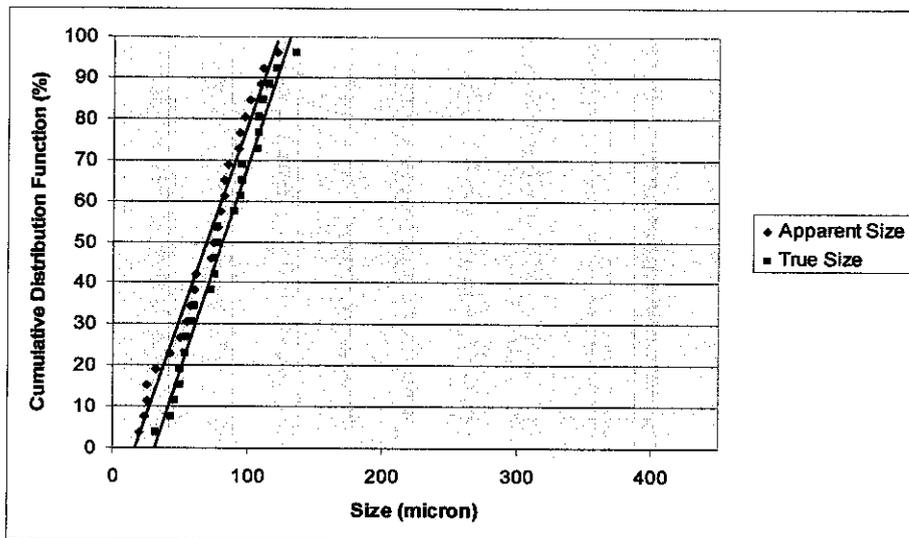
Figure 22: Graph of Weibull Probability using Sample B-1 (Analysis 1)
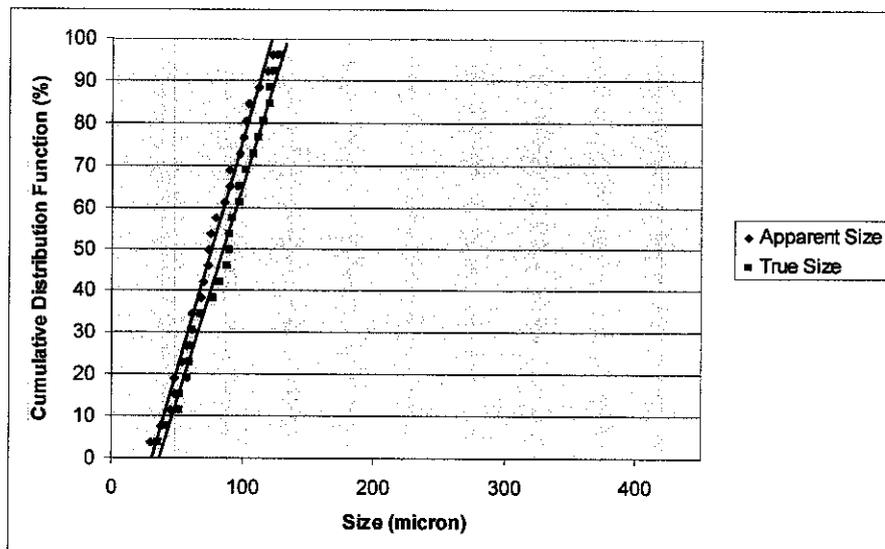
Figure 23: Graph of Weibull Probability using Sample B-1 (Analysis 2)

32
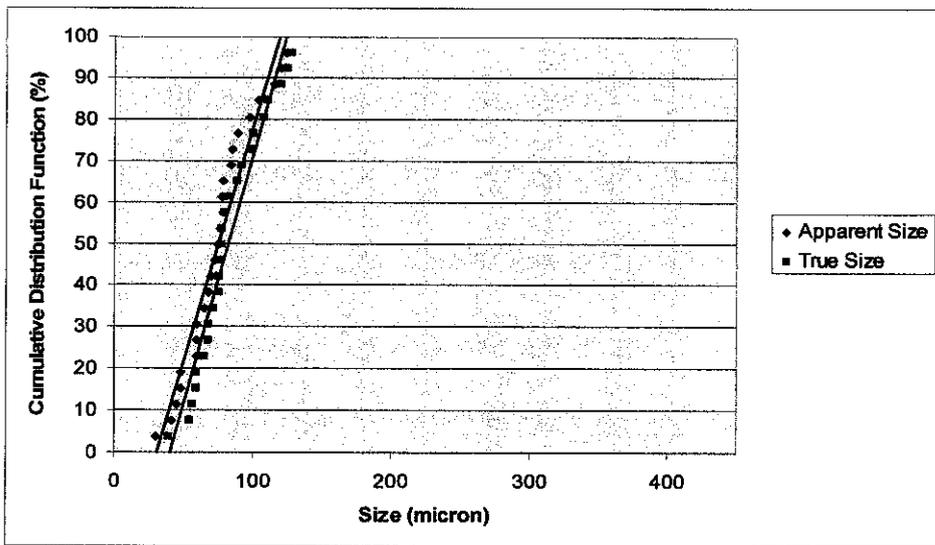
Figure 24: Graph of Weibull Probability using Sample B-2 (Analysis 1)
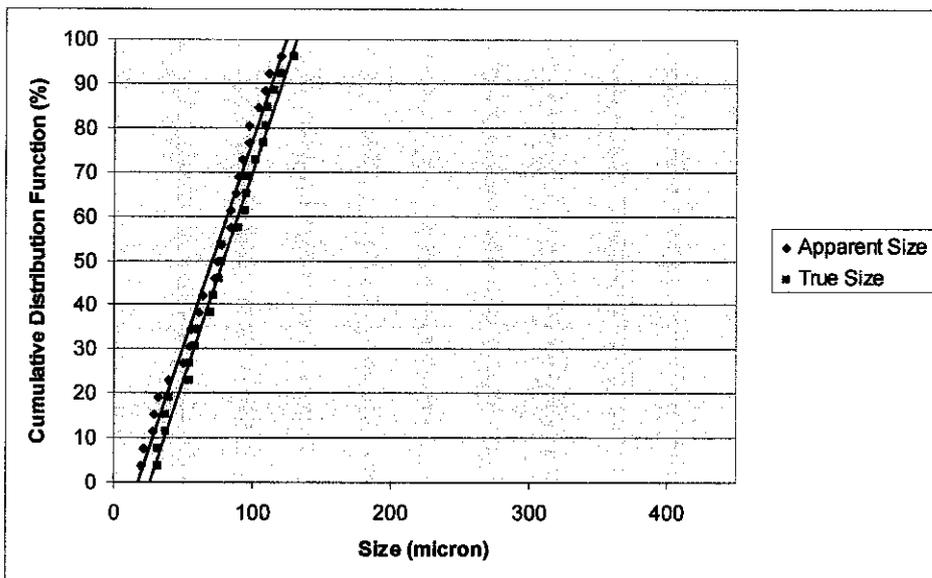
Figure 25: Graph of Weibull Probability using Sample B-2 (Analysis 2)

33
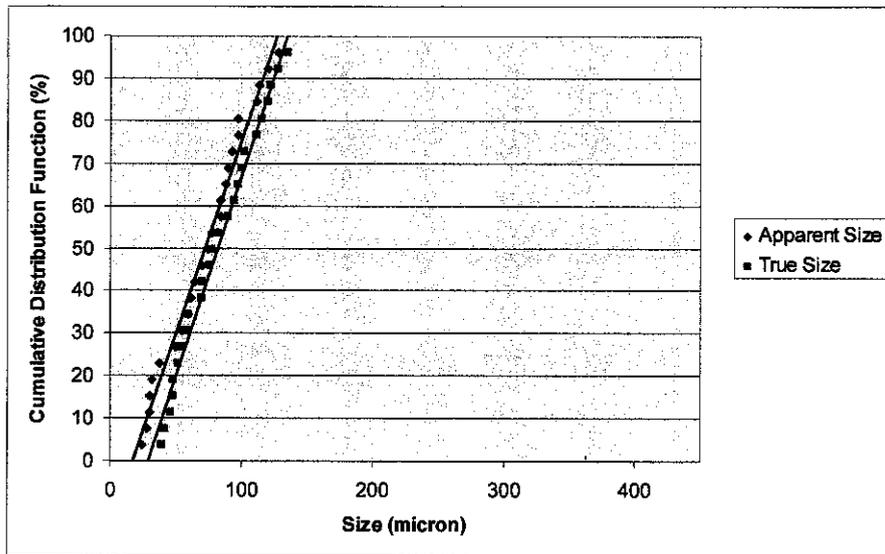
Figure 26: Graph of Weibull Probability using Sample B-2 (Analysis 3)

From Table 4 to Table 8, the average errors are 10.2 percent, 9.5 percent, 16.6 percent, 12.3 percent and 14.3 percent, respectively. From the Figure 17 to Figure 21, all graphs have the two lines with little difference to each other even though the average errors are rather high. This indicates that a mere inspection, without using Weibull probability, or performing low number of inspections, the error will be larger.

Thus, this experiment confirmed that sectioning of sample will have negligible effect on the accuracy of the Weibull probability.

4.3.1 Part C: Data Acquisition & Experiment Work
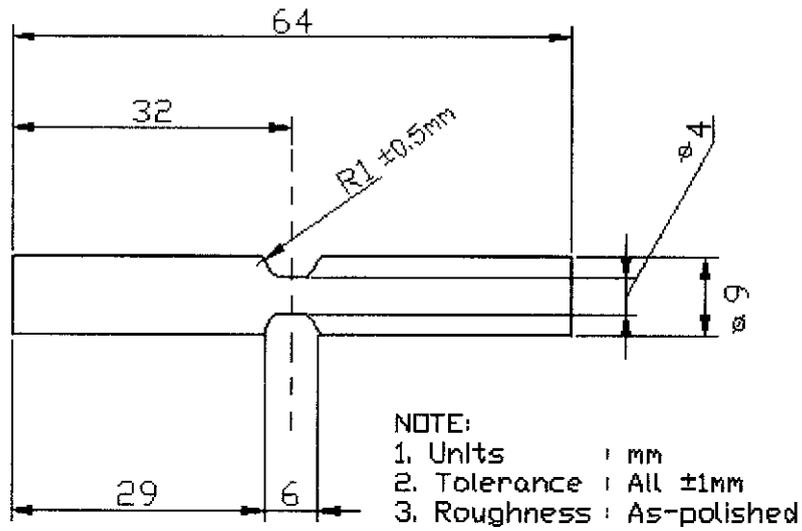
Figure 27: Specimen Dimensions
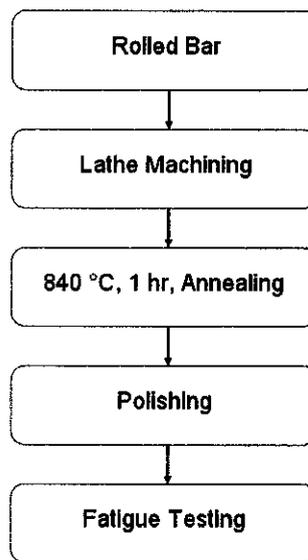
Figure 28: Flow diagram for Specimen Preparation Procedure

Table 7: Chemical Composition (wt%)

Set	C	Si	Mn	P	S
A	0.25	0.22	0.92	0.022	0.031
B	0.27	0.25	0.86	0.018	0.028

Table 8: Rotating Fatigue Test Results

Steel Set	Final Load Applied (N)	Effective Final Load Stress (MPa)	Number of Specimen Failed	Remarks
A HRC 34	5	102.64	0	
	10	205.28	2	
	15	307.92	4	
	20	410.57	2	
	25	513.21	1	
	30	615.15	1	See Note 2
	35	718.49	0	
			Total = 10	
B HRC 35	5	102.64	0	
	10	205.28	1	
	15	307.92	2	
	20	410.57	4	
	25	513.21	2	
	30	615.15	1	See Note 2
	35	718.49	0	
			Total = 10	

Note:

1. Due to lab policy whereby no apparatus can be left on running overnight, the author set the 'run-out' for specimen exceeding 2.52×10^5 cycles. This number is chosen based on 7 hours working time (9.00am to 4.00pm) and rotation speed of 10 Hz.

2. The results should be neglected because at that stress level, it is approaching the ultimate tensile strength of the material, in other words, the material probably had started to yield during the testing setup.

4.3.2 Part C: Discussion

Experiment Validation

Both of the materials used were 0.26 percent carbon steel rolled bar with chemical composition as in the Table 9. By using Energy Dispersive X-ray Spectroscopy, there is no significant dissimilarity in chemical composition; the most important peculiarity is that steel A was obtained from different supplier than steel B.

The specimens were machined into hour-glass-shaped with dimensions as shown in Figure 22. All machined specimens were then undergone annealing at 840 °C, held for 1 hour followed with furnace cooled before being polished. The intention was to force cracks to nucleate internally within the gauge length at oxide inclusions rather than at any other imperfections.

The fatigue test was carried out on HiTech Scientific Rotating Fatigue Machine HSM19mk3 by step-size method. The step-size method is at a test that forces every specimen to fail. This technique is to subject each specimen to a prescribed cycle at each series of increasing stress level, until the specimen fails. The clear advantage is the method saves time and requires fewer specimens.

To start the step-test, initial stress level of 102.64 MPa is selected. The specimen is then tested at that stress level until failure occurs or run-out is achieved, which is at 2.52×10^5 cycles. If failure occurs, the stress level and cycles to failure are recorded. If run-out occurs, the stress level is increased to the next predetermined load. This is repeated until the specimen does fail.

The fractured specimen was inspected, using Scanning Electron Microscope, at the fatigue initiation site for oxide inclusion. Fatigue fracture caused by other factors (i.e. prior crack, defect, cavity, happened outside than gauge length etc) was not taken into account. Hardness test was also performed for each sample set of steel A and steel B, respectively.

Fatigue Test Result

Results of fatigue test are plotted on the Stress Level versus Probability of Failure graph, (see Figure 24) together with best fit line for Set A and Set B using Microsoft Excel.
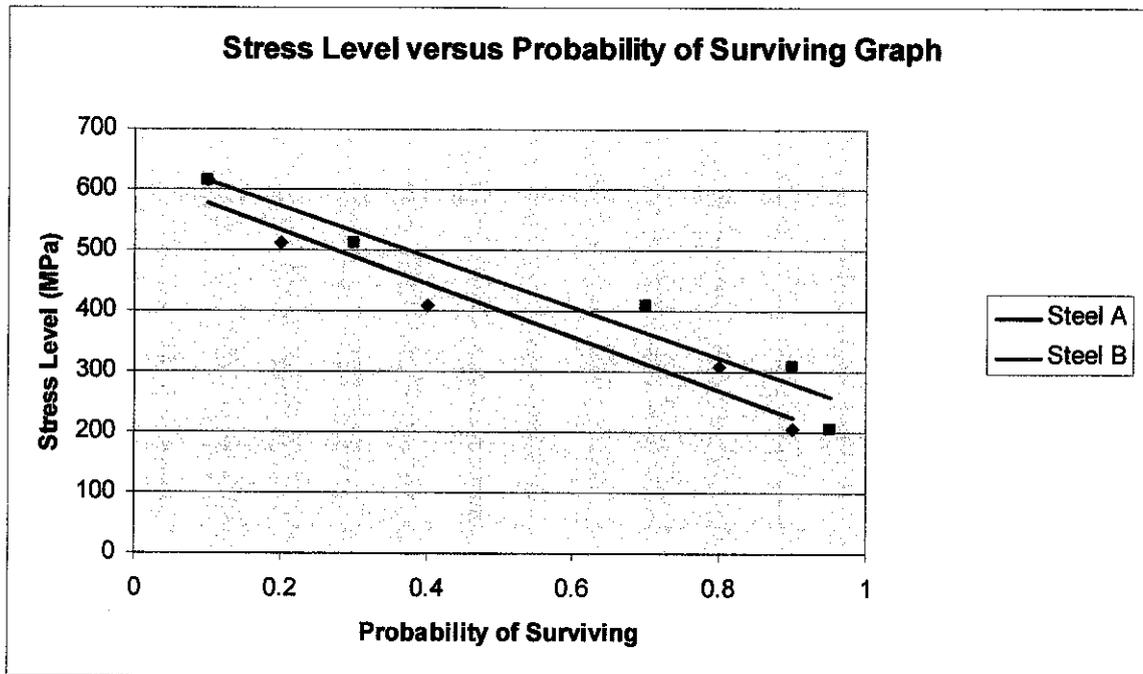
Figure 29: Graph of the Experimental Data

From the graph, it can be seen that Steel B can sustain higher stress level for the same probability of surviving than Steel A. In terms of oxide cleanliness, the Weibull probability is able to point out that Steel B is cleaner than Steel A.

It also confirms the degree of accuracy in predicting the largest inclusion size as close to the actual ones (See Table 9).

Table 9: Comparison between Predicted and Actual Largest Inclusion Size

Set	Predicted Largest Inclusion Size (μm)	Actual Largest Inclusion Size (μm)
A	66	68
B	56	54

CHAPTER 5

CONCLUSION

New approach of determining steel fatigue strength has been proposed by a Japanese group led by Murakami, who developed a method to predict the largest inclusion in a large volume of steel based on observations on metallographic samples [1]. The main objective of this final year project is basically to investigate the feasibility of the proposed method.

In reality, perfect-without-inclusions steelmaking is commercially not feasible. The new approach seems promising to the other steel cleanliness evaluations, which can be seen it the Chapter 4 (Results and Discussions). However, it is worth to note one minor issue associated with this method. The method uses only the largest inclusion in each field of analysis. Hence, many useful data about the *distribution* of large inclusions are being discarded. Clean steel will not be having this problem because largest inclusions are very scarce, let alone to find the distribution of largest inclusion. Other normal steel, on the other hand, is not being used extensively for severe fatigue service condition. Nevertheless, it is worth to further works to address this shortcoming.

As far as this project is concerned, the method is proven through analytical and experimental to have reasonable prediction accuracy of largest oxide inclusion size. Since the author disregarded all specimens that failed other than those because of oxide inclusion, it is sufficed to say that the largest is the ones directly affecting the steel fatigue strength. It is always the largest oxide inclusion found at the origin of the fatigue crack. It is also robust because the technique is not much affected by small deviation due to sectioning.

CHAPTER 6

REFERENCE

[1] Y. Murakami: "Metal Fatigue: Effects of Small Defects and Nonmetallic Inclusions", Kyushu University, Tokyo (2002).

[1a] J. Monnot, B. Heritier and J.Y. Cogne: "Relationship of Melting Practice, Inclusion Type, and Size with Fatigue Resistance of Bearing Steels", ASTM STP 987 (1998).

[1b] A. Adachi, H. Shoji, A. Kuwabara & Y. Inoue: "Rotating Bending Fatigue Phenomenon of JIS SUJ2 Bearing Steel", Electr. Furnace Steel, 46(3) (1975).

[1c] Y. Murakami, T. Toriyama and E.M. Coudert: "Instructions for New Methods of Inclusion Rating and Correlation with the Fatigue Limit", J. Testing Evaluation (1994).

[1d] L.O. Uhrus: "Through-Hardening Steels for Ball Bearings - Effect of Inclusions on Endurance", Iron Steel Institute, Spec. Rep. 77 (1963).

[1e] W.E. Duckworth & E. Ineson: "The Effects of Externally Induced Alumina Particles on the Fatigue Life of EN24 Steel", Clean Steel, Iron Steel Institute Spec. Rep 77 (1963).

[1f] F. de Kazinczy: "Effect of Small Defects on the Fatigue Properties of Medium-Strength Cast Steel", J. Iron Steel Institute, 208 (1970).

[1g] Y. Murakami, Y. Uemura & K. Kawakami: "Some Problems in the Application of Statistics of Extreme Values to Estimation of the Maximum Size of Nonmetallic Inclusions in Metals", Trans. Jpn. Soc. Mech. Eng. A, 55 (509) (1989), 58-62.

[2] A. J. McEvily: "Metal Failures: Mechanism, Analysis, Prevention", John-Wiley & Sons, USA (2002).

[3] J. J. C. Hoo & W. B. Green Jr.: "Bearing Steels: Into 21st Century", ASTM, STP 1327, USA (1998).

[4] T. Lund & P. Olund: "Development of Clean Steels – Advantages in Ladle Metallurgy and Testing Technology", Technical Report 1/2000, Ovako Steel.

[5] T. Hansen: "Some Ideas of Determining the Macro Inclusion Characteristics during Steelmaking", MEFOS, Sweden.

[6] "Standard Test Methods for Determining the Inclusion Content of Steel", ASTM E45 - 97 (Re-Approved 2002), Pennsylvania, USA, Section 5.1.2 (Fracture Test).

[7] Kiessling, R.: "Non-metallic Inclusions in Steel: Part V", Institute of Metals of London & Institute of Metals USA (1989).

[8] Stolte, G.: "Secondary Metallurgy: Fundamentals Processes Applications", Verlag Stahleisen GmbH, Dusseldolf, Germany (2002).

[9] Briant, C. L.: "Impurities in Engineering Materials: Impact, Reliability and Control", CRC Press (1999).

[10] Petronas Penapisan Terengganu: "Introduction to Metallurgy", PDF format.

[11] "Clean Steel: Superclean Steel", edited by J. Nutting & R. Viswanathan, Conference of The Institute of Materials on behalf of The Electric Power Research Institute, California, USA (6 - 7 March 1997, London, UK), The University Press Cambridge UK (1996).

[11a] J.H. Lowe & A. Mitchell, "Zero Inclusion Steels", Axel Johnson Metals Corporation (USA) & Dept of Metals and Materials Engineering, University of British Columbia (Canada).

[11b] J. Dijk, D. Manneveld & J.M. Rabenberg: "Proc. 4th International Conference on Clean-Steels, Balatonszeplak, Hungary (1992), Institute of Materials.

[12] "Impurities in Engineering Materials: Impact, Reliability and Control", edited by Clyde L. Briant, Brown Unversity Providence, Rhode Island, Marcel Dekker Inc. (1999).

[13] Alok Nayar: "Testing of Metals", Materials Engineering and Metrology, Faridabad, India, Tata McGraw-Hill Publishing New Delhi (2005).

[13a] IS 4163:1982, "Method for Determination of Inclusion Content in Steel by Microscopic Method".

[13b] ISO 4967:1998, "Steel - Determination of Content of Nonmetallic Inclusions - Micrographic Method Using Standard Diagrams".

[13c] ASTM E45:1997, "Standard Test Methods for Determining the Inclusion Content of Steel".

[13d] IS 10138:1992, "Macroscopic Methods for Determination of Non-metallic Inclusion Content in Wrought Steels - Part 1: Blue Fracture Test Method.

[13e] IS 3763: 1976, "Wrought Steels - Macroscopic Methods for Assessing the Content of Non-Metallic Inclusions".

[13f] K.E. Thelning: "Steel and Its Heat Treatment, 2nd Edition, Butterworths, London, UK (1984).

[14] Sheldon M. Ross: "Introduction to Probability and Statistics for Engineers and Scientists:, 3rd Edition, Department of Industrial Engineering and Operations Research, University of California, Berkeley, Elvesier Academic Press (2004).

[15] D.C. Montgomery, G.C.Runger & N.F. Hubele: "Engineering Statistic", 4th Eition, Arizona State University, John Wiley & Sons (2007).

[16] Jack A. Collins: "Failure of Materials in Mechanical Design: Analysis, Prediction, Prevention", 2nd Edition, The Ohio State University, Columbus, John Wiley & Sons, p379-381(1993).

[16] M. Endo: "Effects of Small Defects on the Fatigue Strength of Steel and Ductile Iron under Combined Axial / Torsional Loading", Dept. of Mechanical Eng., Fukuoka University, Japan.

[17] K.S. Ravichandran, R.O. Ritchie & Y. Murakami (editors): "Small Fatigue Cracks: Mechanics, Mechanisms and Applications", proceedings of the Third Engineering International Conference, Elsevier Science Ltd. (1999).

APPENDICES

Fatigue Testing (Step-Test Method)

Stress (MPa)

615.15

513.21

410.57

307.92

205.28

102.64

Failure

X

O

Number of Cycle to Failure (N)

10^2 10^3 10^4 10^5 10^6

Stress (MPa)

615.15

513.21

410.57

307.92

205.28

102.64

Failure

X

O

O

Number of Cycle to Failure (N)

10^2 10^3 10^4 10^5 10^6

Stress (MPa)

615.15	
513.21	X ← Failure
410.57	o
307.92	o
205.28	o
102.64	o

Number of Cycle to Failure (N)

10²   10³   10⁴   10⁵   10⁶

Stress (MPa)

615.15	
513.21	
410.57	X ← Failure
307.92	o
205.28	o
102.64	o

Number of Cycle to Failure (N)

10²   10³   10⁴   10⁵   10⁶